

Environmental Science Nano

Accepted Manuscript



This is an *Accepted Manuscript*, which has been through the Royal Society of Chemistry peer review process and has been accepted for publication.

Accepted Manuscripts are published online shortly after acceptance, before technical editing, formatting and proof reading. Using this free service, authors can make their results available to the community, in citable form, before we publish the edited article. We will replace this *Accepted Manuscript* with the edited and formatted *Advance Article* as soon as it is available.

You can find more information about *Accepted Manuscripts* in the [Information for Authors](#).

Please note that technical editing may introduce minor changes to the text and/or graphics, which may alter content. The journal's standard [Terms & Conditions](#) and the [Ethical guidelines](#) still apply. In no event shall the Royal Society of Chemistry be held responsible for any errors or omissions in this *Accepted Manuscript* or any consequences arising from the use of any information it contains.

Nano Impact Statement:

Nanoparticle synthesis mechanisms are difficult to study given the fast rate of the physicochemical processes involved in the nucleation and growth of nanoparticles. A deeper mechanistic understanding will allow us to develop design rules for synthesizing nanoparticles with tightly controlled sizes and morphologies. Moreover, we need to incorporate principles of green chemistry and engineering into those design rules to improve conventional energy-intensive nanomaterial production practices. This paper describes the synthesis of citrate-reduced gold nanoparticles at room temperature. This method allows us to probe the mechanisms involved therein, as well as reduces the life cycle environmental impacts of the production step. The mechanistic insights gained from this study can inform new green synthesis approaches for producing other nanomaterials.

(117 Words)

ROOM TEMPERATURE SEED MEDIATED GROWTH OF GOLD NANOPARTICLES: MECHANISTIC INVESTIGATIONS AND LIFE CYCLE ASSESMENT

*Weinan Leng, Paramjeet Pati, and Peter J Vikesland **

Department of Civil and Environmental Engineering, Virginia Polytechnic Institute and State University, 418 Durham Hall, Blacksburg, VA 24060-0246

*Corresponding author e-mail address: pvikes@vt.edu

Abstract

In this study, we report the first room temperature seed-mediated synthesis of gold nanoparticles (AuNPs) in the presence of citrate and gold salt. In contrast to citrate-reduction in boiling water, these mild reaction conditions provide expanded capacity to probe the mechanism of seed-mediated growth following gold salt addition. Moreover, comparative life cycle assessment indicates significant reductions in the environmental impacts for the room temperature synthesis. For this study, highly uniform gold seeds with Z-average diameter of 17.7 ± 0.8 nm and a polydispersity index of 0.03 ± 0.01 were prepared by a pH controlled protocol. We investigated the AuNP growth mechanism via time resolved UV-vis spectroscopy, dynamic light scattering, and transmission electron microscopy. This study indicates that citrate and its oxidation byproduct acetone dicarboxylate serve to bridge and gather Au(III) ions around gold nanoparticle seeds in the initial growth step.

Key words: Room temperature; seed-mediated growth; gold nanoparticles; life cycle assessment

INTRODUCTION

Nanotechnology holds immense promise for its capacity to address many societal problems. A key challenge in exploiting the novel properties of nanomaterials is in the synthesis of nanoparticles with precisely controlled sizes and morphologies. In addition, nanomaterial synthesis may involve multi-step, multi-solvent, energy intensive manufacturing processes^{1, 2} that may be associated with significant environmental impacts. Recently there have been

31 increased efforts 1) to develop design principles to synthesize highly monodisperse
32 nanoparticles^{3, 4} and 2) to incorporate the principles of green chemistry into nanomaterial
33 synthesis.⁵⁻⁷ In this paper we present a novel approach for the room temperature seeded growth
34 of gold nanoparticles (AuNPs) and compare its life cycle impacts with those of previously
35 reported methods^{8,9} that require high-temperature boiling.

36 AuNPs and their conjugates are particularly versatile nanomaterials.¹⁰⁻¹² Exhibiting low
37 toxicity in biological systems,¹³⁻¹⁵ AuNPs conjugated with drugs and peptides have been used to
38 modulate pharmacokinetics and drug delivery, thus allowing for specific targeting of cancer cells
39 and organelles.¹⁶⁻²¹ The physical properties of AuNPs (e.g., color, localized surface plasmon
40 resonance (LSPR), electrical conductivity, etc.) are significantly enhanced when they are
41 functionalized with appropriate metal or organic groups.²² For example, aggregation induced
42 changes in plasmon response can be coupled with colorimetric detection mechanisms to establish
43 rapid analyte detection.^{13, 23-27} Such methods are promising in that they entail very simple sample
44 handling procedures, minimum instrumental investment, and can be carried out in the field using
45 portable devices.

46 The nanoscale properties of AuNPs are size- and shape-dependent,^{11, 28} and thus there has
47 been an extensive effort to control AuNP size, shape, and surface composition while
48 simultaneously maintaining narrow size distributions.^{11, 29-32} The synthesis of gold nanoparticles
49 by trisodium citrate (Na₃Ctr) mediated reduction of aqueous chloroauric acid (HAuCl₄)^{8,9}, is one
50 of the most widely used AuNP synthesis strategies. This synthesis approach, involving rapid
51 addition of Na₃Ctr into a hot aqueous solution of HAuCl₄, has been modified and optimized over
52 many decades.^{31, 33-35} In this synthesis Na₃Ctr simultaneously acts as (i) reducing agent (driving
53 the reduction of Au^{III} to Au⁰),^{9, 33, 36, 37} (ii) capping agent (electrostatically stabilizing the AuNP
54 colloidal solution),³⁷⁻³⁹ and (iii) pH mediator (modifying the reactivity of Au species involved in
55 the reaction).³¹

56 Room temperature syntheses of noble metal nanoparticles involving synthetic surfactant⁴⁰
57 and bio-based reductants and capping agents⁴¹ have been previously reported. Seed-mediated
58 growth of AuNPs has been shown to be especially effective in producing highly monodisperse
59 AuNPs.^{42, 43} In this work, however, we discuss what we believe to be the first effort to examine
60 seed-mediated AuNP growth in the presence of citrate and gold salt at room temperature. Highly
61 uniform and reproducible gold seeds were prepared for seed-mediated growth using a pH-

62 controlled protocol. By inoculating the growth medium with a controlled number of gold seeds,
63 the particles produced via this approach have sizes varying from 20-110 nm with the final size
64 dependent on the number of seeds and the total concentration of gold ions in the growth solution.
65 Given the room temperature conditions, this seeded growth synthesis approach adheres to
66 Principle 6 of the Green Chemistry Principles⁴⁴ (Design for Energy Efficiency), which
67 recommends using ambient temperature and pressure whenever possible. The longer reaction
68 times also offer new opportunities to probe the reaction mechanism and study the evolution of
69 AuNP size and morphology.

70 Sustainability has been identified as an emerging design criterion in nanomaterial synthesis.³
71 Incorporating green chemistry and engineering principles into nanoscience has been suggested as
72 a proactive approach to mitigate the environmental impacts of nanotechnology.^{5, 6} However,
73 green synthesis approaches for nanoparticle production may have unintended environmental
74 impacts.⁴⁵ Life cycle assessment (LCA) is being increasingly used to study the environmental
75 impacts of different nanotechnologies to assess tradeoffs and identify environmental hotspots
76 therein.⁴⁶⁻⁵⁰ For example, are reductions in the energy footprint of the AuNP synthesis process
77 due to the milder room temperature conditions substantially larger than any increase in the
78 energy use due to longer reaction times? To investigate this issue, we conducted an LCA study to
79 compare the environmental impacts of the AuNP synthesis at room temperature as well as under
80 boiling conditions.

81

82 MATERIALS AND METHODS

83 **Materials.** Gold(III) chloride trihydrate ($\text{HAuCl}_4 \cdot 3\text{H}_2\text{O}$) and trisodium citrate dihydrate
84 ($\text{Na}_3\text{Citr} \cdot 2\text{H}_2\text{O}$) were purchased from Sigma-Aldrich (St. Louis, MO) at the highest purity grade
85 available. Deionized water (18 M Ω -cm) was used for all preparations. All glassware was cleaned
86 in a bath of freshly prepared aqua regia (HCl/HNO_3 , 3:1 v/v) and then rinsed thoroughly with
87 deionized water prior to use. All reagent solutions were filtered through a 0.2 μm polycarbonate
88 membrane prior to their use in AuNP synthesis.

89 **AuNP seed preparation.** Gold nanoparticles of ≈ 14 nm diameter were synthesized according
90 to Frens *et al.*⁸ with a slight modification for size and monodispersity control.³¹ This synthesis
91 involves chemical reduction of AuCl_4^- at pH 6.2–6.5 by dissolved Na_3Citr at 100 °C. In brief, 100
92 mL of 1 mM HAuCl_4 containing 200 μL of 1 M NaOH was prepared in a 250-mL flask equipped

93 with a condenser. The solution was brought to boil while being stirred with a PTFE-coated
94 magnetic stir-bar and 10 mL of 38.8 mM Na₃Ctr was rapidly added. The reaction was allowed to
95 proceed until the solution attained a wine red color. After 15 min of reaction, the reflux system
96 was shut down and deionized water was added to the AuNP seed suspension to bring the final
97 volume to \approx 100 mL. ‘Room temperature synthesis’ as used herein refers explicitly to the seed-
98 mediated growth of AuNPs and not the synthesis of AuNP seeds. We utilized elevated
99 temperatures for seed production as we found it to be the best way to control the monodispersity
100 of the seeds. We note, however, that citrate-stabilized AuNP seeds may be synthesized by other
101 methods that may or may not involve elevated temperatures.

102 ***Seed-mediated AuNP growth at room temperature.*** Growth reactions (40 mL final volume)
103 were performed in a 100-mL Erlenmeyer flask. Briefly, a variable volume aliquot of seed
104 suspension ($N = 6.54 \times 10^{12}$ particles/mL) and 227 μ L of 44.7 mM HAuCl₄·3H₂O were added to
105 the flask with water. Subsequently, a 176 μ L aliquot of 38.8 mM Na₃Ctr·2H₂O was added to the
106 flask under constant stirring. In these syntheses the only variable was the initial AuNP seed
107 concentration (Supporting Information Table S1).

108 ***AuNP characterization.*** UV–vis spectra were acquired using a Cary 5000 UV-vis-NIR
109 spectrophotometer. AuNP suspensions were placed in 1 cm sample cells and spectra between
110 400-800 nm were acquired at room temperature. For the time-dependent measurements of the
111 seeded growth experiments, aliquots were removed and samples were probed within 2 min of
112 reductant addition. At the same time, an aliquot of suspension was frozen at -20 °C. At this
113 temperature the suspended nanoparticles precipitated out of the suspension. The thawed solution
114 was centrifuged at 10000 \times g for 10 min, and the supernatant was used for UV-vis and ICP-MS
115 analysis.

116 Gold nanoparticles were visualized using a Zeiss 10CA transmission electron microscope
117 equipped with an AMT Advantage GR/HR-B CCD Camera System. Sample aliquots of 3 μ L
118 were drop-cast onto carbon-coated 100-mesh copper grids (Electron Microscopy Sciences). After
119 5 minutes, the drop was wicked away using filter paper. The sample was then rinsed three times
120 by inverting the TEM grid onto a drop of water for 5 seconds and then allowing the grid to dry
121 face up. TEM images of the as prepared AuNPs were used for size distribution measurements.
122 For each sample, the dimensions of >60 particles were quantified using NIH ImageJ software
123 (version 1.44). Electrophoretic mobility and intensity based particle size distributions and

124 hydrodynamic diameter were determined with a Zetasizer NanoZS instrument (Malvern
125 Instruments, UK) with a 173° scattering angle at a temperature of 25 °C. A refractive index of
126 1.35 and an absorption value of 0.01 were used for the AuNPs.⁵¹ Raman experiments were
127 performed using a WITec alpha500R (Ulm, Germany). A 10× Olympus objective (NA=0.3) was
128 used to focus a 633 nm laser into a 2-mm flow cell. The Raman signal was collected using a 30s
129 integration time.

130 **Size and concentration calculation of AuNPs.** (1) *Size and concentration of Au seeds.* The
131 average size of the gold seeds was calculated via TEM analysis. A TEM image of seeds
132 synthesized via the pH controlled method is shown in Figure 1. Using ImageJ, the average
133 nanoparticle diameter (d_{seed}) was determined to be 13.9 ± 0.5 nm. Assuming a spherical particle
134 and a reaction yield of 100%,⁴⁵ the number density of gold seeds ($N_{seed} = 6.75 \times 10^{12}$ particles/mL)
135 was calculated based upon the known initial concentration of gold c_{Au} (mol/L):⁵²

$$136 \quad N_{seed} = \frac{6 \times 10^{21} c_{Au} M}{\pi \rho_{Au} d_{seed}^3} \quad (1)$$

137 where ρ is the density of gold (19.3 g/cm³) and M is its atomic weight (197 g/mol). A similar
138 concentration of 6.54×10^{12} particles/mL was calculated based upon the absorbance of the particle
139 suspension at 450 nm (A_{450}) using the method reported by Haiss *et al.*⁵³

$$140 \quad N_{seed} = \frac{A_{450} \times 10^{14}}{d_{seed}^2 \left[-0.295 + 1.36 \exp\left(-\left(\frac{d_{seed}-96.8}{78.2}\right)^2\right) \right]} \quad (2)$$

141 Given the similarity of these values and due to the possibility of overestimating the gold
142 nanoparticle concentration following filtration, a N_{seed} value of 6.54×10^{12} particles/mL as
143 determined using the Haiss equation was used in all calculations.

144 (2) *Size and concentration of seed mediated AuNPs.*

145 Assuming that (a) all of the gold precursor is consumed during the reaction, (b) the resultant
146 AuNPs are spherical in shape, and (c) gold reduction and nanoparticle growth take place without
147 nucleation of new ‘seed’ particles, the effective size of the grown particles can be quantitatively
148 predicted.⁵⁴

$$149 \quad d_{AuNP}^3 = d_{seed}^3 + \frac{6 \times 10^{21} m_{Au}}{\pi \rho_{Au} n_{seed}} \quad (3)$$

150 Where m_{Au} and n_{seed} are the Au mass (g) and the number of seed particles present during seed
151 mediated growth. The number density of AuNPs (N_{AuNP}) is simply n_{seed} divided by the total
152 volume (V) of the AuNP solution,

$$N_{AuNP} = \frac{n_{seed}}{V} \quad (4)$$

154 The molar concentration of the AuNP solutions was then calculated by dividing the number
155 density of particles by Avogadro's constant (6.022×10^{23}).

156 ***Life cycle assessment (LCA) of AuNP synthesis methods.*** LCA is a quantitative framework
157 used to evaluate the cumulative environmental impacts associated with all stages of a material –
158 from raw material extraction through the end-of-life.⁵⁵ We conducted a cradle-to-gate
159 comparative LCA of seeded-AuNP growth at room temperature and under boiling conditions.
160 Our LCA models consider processes from raw material extraction (“cradle”) and processing
161 through the synthesis of the nanoparticles (“gate”). The functional unit is 1 mg of AuNP
162 synthesized by each approach. The LCA models exclude purification steps and synthesis waste
163 products. Furthermore, we did not consider recycle streams since it is not common practice to
164 capture AuNP waste streams in laboratory scale synthesis.

165 The material and energy inventories for the AuNP synthesis were built using measured data
166 from our laboratory. The average medium-voltage electricity mix for the US Northeast Power
167 Coordinating Council was used to model energy use. The uncertainty for energy use was
168 modeled as a uniform distribution with the maximum and minimum values being $\pm 20\%$ of the
169 calculated energy use as per measurements performed in our laboratory. LCA models were
170 constructed using SimaPro (version 8.0.4). The inventory for chemical precursors used in these
171 syntheses was modeled using the EcoInvent database⁵⁶ (version 3.01).

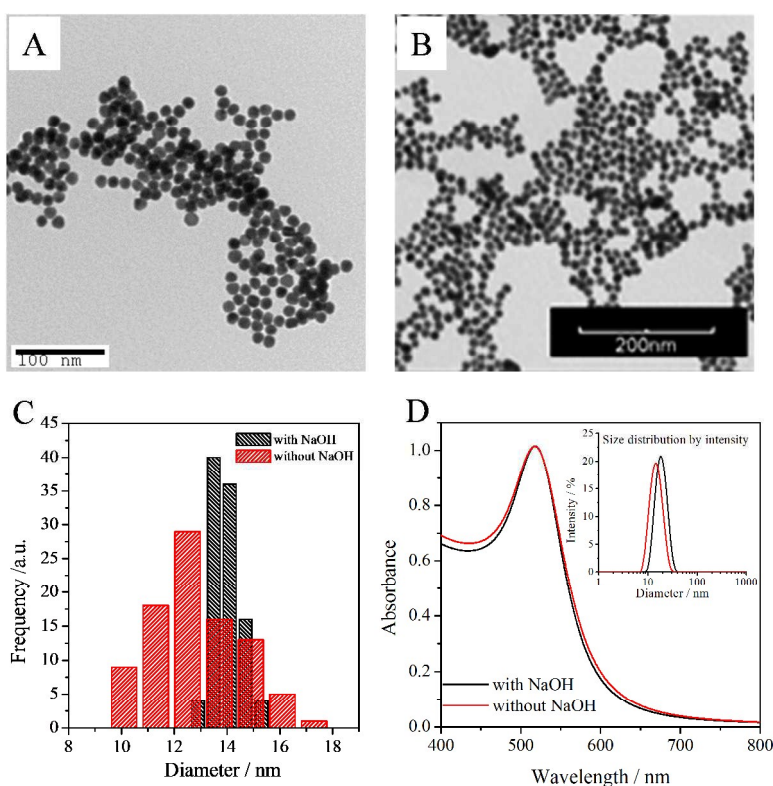
172 Gold(III) chloride and sodium citrate were not found in the LCA inventory databases.
173 Therefore, the synthesis of these two chemicals were modeled as custom-built processes using
174 appropriate assumptions for yield and uncertainties as discussed elsewhere (Table S2).⁵⁷ Life
175 cycle impact assessment (LCIA) was done using the Cumulative Energy Demand (CED)
176 method^{56, 58} (version 1.09) and the ReCiPe MidPoint method (version 1.11), using midpoints and
177 the hierarchist (H) perspective with European normalization. CED estimates the embodied and
178 direct energy use for materials and processes in the syntheses and gives a detailed energy
179 footprint. The ReCiPe impact assessment method estimates life cycle impacts across a broad
180 range of impact categories (e.g., climate change, freshwater eutrophication, marine ecotoxicity,
181 etc.). All uncertainty analyses were performed using Monte-Carlo simulations for 1000 runs.
182 The uncertainty analyses include the uncertainties in the custom-defined processes in SimaPro,
183 energy use in lab equipment and the unit processes in EcoInvent used in our LCA models.

184 Figures S1 and S2 show the chemicals and processes considered in the LCA models. The life
185 cycle inventories are shown in Tables S2, S3, and S4.

186

187 RESULTS AND DISCUSSION

188 **Monodisperse AuNP seed production.** Highly uniform and reproducible AuNP seeds were
189 prepared via citrate reduction both with and without pH adjustment. In the traditional
190 Turkevich/Frens' approach, nanoparticle size, nanoparticle polydispersity, and the overall
191 reaction mechanism are determined by the solution pH set by $[\text{Na}_3\text{Cit}]$.³¹ Unfortunately, as the
192 $\text{Na}_3\text{Cit}/\text{HAuCl}_4$ ratio increases from 0 to 30 there is an increase in solution pH from 2.8 to 6.8
193 (Figure S3, Supporting Information). Over this pH range, AuCl_4^- undergoes pH-dependent
194 hydrolysis to produce $[\text{AuCl}_x(\text{OH})_{4-x}]^-$ ($x=0-4$) complexes.⁵⁹ Due to the electron withdrawing
195 capacity of the hydroxyl ligand increased gold ion hydroxylation results in an increase in



196
197 Figure 1. TEM micrographs of seed nanoparticles synthesized by (A) pH controlled method and
198 (B) w/o pH control; (C) TEM size distributions from both methods; (D) Normalized absorption
199 spectra and hydrodynamic size distribution by intensity (Inset) of two seed suspensions with
200 (black lines) and w/o pH controlled (red lines) procedures. Suspensions were diluted 3× and 9×
201 for UV-vis and DLS measurements, respectively.

202

203 standard reduction potential (Figure S4, Supporting Information).^{31, 60, 61} Past studies have shown
204 that the final AuNP size can be tuned by changing the solution pH due to this effect.^{31, 60}

205 Addition of Na₃Ctr without pH control causes the solution pH to increase above 6.2 during
206 the latter stages of AuNP synthesis. This change converts highly reactive AuCl₃(OH)⁻ into less
207 reactive complexes of AuCl_X(OH)_{4-X} (X=0-2), and the reaction pathway consists of a single
208 nucleation-growth step.^{31, 61} Tight control of nanoparticle size is challenging under these
209 conditions because growth and nucleation occur simultaneously during the early stages of Na₃Ctr
210 addition (i.e., when the pH < 6.2). To address this issue during seed preparation we set the
211 solution pH to a value of ≈6.4 by addition of 200 μL of 1 M NaOH to the reaction solution.

212 Figure 1A shows a typical TEM micrograph for seed nanoparticles synthesized using our pH
213 controlled synthetic protocol. The nanoparticles are highly monodisperse with a pseudo-spherical
214 diameter of 13.9 ± 0.5 nm and an average aspect ratio (AR) of 1.06 ± 0.04. We also calculated
215 average particle diameters using Haiss' equation 11 (with B₁=3.00 and B₂=2.20),⁵³ based on the
216 UV-vis spectra of the AuNP seeds. This particle diameter (13.6 ± 0.7 nm) closely matched the
217 average particle size obtained from TEM measurements (13.9 ± 0.5 nm). The size distribution of
218 3.6% coincides with a highly reproducible DLS Z-average diameter and polydispersity index
219 (PDI), 17.7 ± 0.8 nm and 0.03 ± 0.01, respectively, for twelve replicate batches. Particles
220 synthesized without pH control (i.e., without adding NaOH) were also characterized (as
221 illustrated in Figure 1). For this synthesis, the pH value of 5.6 at the beginning of reaction was
222 set by the Na₃Ctr/HAuCl₄ ratio alone (Figure S3, Supporting Information). Compared with the
223 pH controlled synthesis, an immediate color change (< 1 min) of the reaction suspension was
224 observed following Na₃Ct injection, while the pH controlled reaction required 2-3 min to see a
225 similar color change, thus indicating faster nucleation and growth due to the higher reactivity of
226 the gold complexes at elevated pH (Figure S4, Supporting Information). Although Figure 1D
227 shows the two syntheses have very similar LSPR λ_{max} (517.9 nm for non pH controlled particles,
228 518.5 nm for pH controlled particles), the hydrodynamic diameter and TEM diameter of the
229 nanoparticle increased from 15.2 nm to 17.7 nm and from 12.9 nm to 13.9 nm respectively as the
230 pH increased from 5.6 to 6.4. Consistent with the broader TEM size distribution (Figure 1C) and
231 absorption peak width at half maximum⁶² of the LSPR band (Figure 1D), a larger PDI of 0.19
232 was obtained for the non-pH controlled particles along with a 17% error between the particle size
233 determined based upon the TEM measurements (12.9 nm) and the size calculated using the Haiss

234 equation (10.7 nm). As the initial Au^{III} concentration and the Na₃Ct/HAuCl₄ ratio were both
235 fixed for the two seed synthesis approaches, this finding is consistent with the previous
236 observation that AuNP size and monodispersity of gold nanocrystals are strongly dependent on
237 the initial pH of the reaction medium.³¹

238 **Room temperature seeded growth of AuNPs.** Because of the rapid reaction kinetics at 100
239 °C it is necessary to keep Au^{III} and the reductant apart during seed-mediated growth⁶³ and the
240 order and speed of reagent addition strongly affect the final size and polydispersity of the
241 nanoparticles.⁶² To achieve improved nanoparticle homogeneity, we hypothesized that seeded
242 growth could be carried out at room temperature – and could simply be initiated following
243 addition of seed nanoparticles to premixed solutions of Au^{III} and reductant (or alternatively the
244 introduction of Au^{III} to a mixture of reductant and seeds). As illustrated herein, such an outcome
245 can be accomplished when the rate constant for surface mediated growth is significantly greater
246 than the rate constant for nucleation – a condition that occurs at room temperature. As shown in
247 Figure 2, by inoculating the growth medium with a controlled number of gold seeds, the particles
248 produced via this approach have sizes varying from 20-110 nm with the final size dependent on
249 the number of seeds and the total concentration of gold ions in the growth solution. A majority of
250 the NPs produced by this approach are quasi-spherical in shape, although nanocrystal triangles
251 and rods also form in low yield (<13%) in the larger nanoparticle (>70 nm) preparations (Table
252 S5). Ignoring the presence of the non-spherical particles, the average diameters and
253 concentrations of the particles were determined and are tabulated in Table 1. For this calculation,
254 we assumed that all of the particles exhibit spherical geometries. However, as illustrated in
255 Figure 2 this assumption becomes increasingly incorrect for the larger nanomaterial sizes. We
256 note that the similarity in particle size determined experimentally and predicted using equation (3)
257 suggests that nucleation of small nanoparticles does not occur, thus indicating that the final
258 concentration of AuNPs correlates well with the initial number of AuNP seeds.

259 As indicated in Table 1 and Figure S6A, we determined the hydrodynamic diameter and size
260 distribution of the AuNPs using DLS. The extreme sensitivity of the scattered signal to changes
261 in the radius (R) of the scattering objects (scattered intensity $\propto R^6$),⁶⁴ enables DLS to detect the
262 presence of even small numbers of aggregates in NP dispersions. The seeded AuNPs in our work
263 are not true spheres and should be described as ovoid with one dimension elongated relative to
264 the other. The effects of rotational diffusion result in the appearance of a false peak in a size

265 Table 1. Sizes, concentrations, zeta-potentials, and optical properties of seeded AuNPs

AuNP	SPR peak (nm)	Concentration (NPs/mL) ^a	Mean ξ potential (mV)	Diameter of AuNP (nm)		
				Calculated ^b	TEM ^c	Z-average/PDI (DLS)
A	525.9	5.5×10^{11}	-40.5 \pm 1.2	22.7	24.0 \pm 6.1	25.9/0.193
B	533.9	1.3×10^{11}	-40.2 \pm 0.7	34.2	37.1 \pm 4.6	25.0/0.53
C	536.5	5.4×10^{10}	-38.7 \pm 1.1	45.7	46.0 \pm 4.6	31.2/0.502
D	537.2	2.7×10^{10}	-40.7 \pm 1.6	57.1	57.6 \pm 4.5	45.9/0.314
E	541.2	1.6×10^{10}	-42.7 \pm 0.5	68.6	69.6 \pm 11.8	61.2/0.239
F	551.9	9.7×10^9	-43.5 \pm 0.6	80.0	82.5 \pm 14.0	79.2/0.162
G	561.2	6.5×10^9	-44.4 \pm 1.5	91.4	92.4 \pm 11.4	89.7/0.148
H	569.9	4.6×10^9	-42.2 \pm 2.7	102.9	100.0 \pm 11.4	97.8/0.113
I	581.9	3.3×10^9	-46.6 \pm 1.4	114.3	111.0 \pm 8.3	105.8/0.114

266 ^aTheoretical concentration of seeded AuNPs based upon the seed concentration and assuming
 267 that all gold salt precursors are reduced to gold atoms that condense onto the seed particle
 268 surface;

269 ^bParticle sizes as determined using Eq 3 for a seed concentration of 6.54×10^{12} particles / mL.

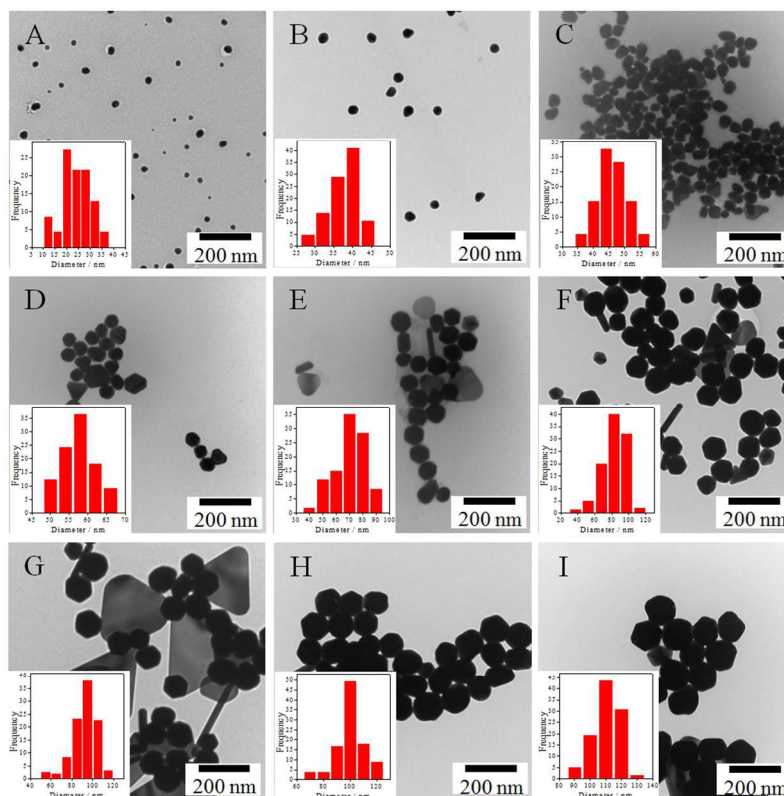
270 ^cFor the particles with one dimension elongated, the sizes are overestimated by
 271 $[(AR)^{1/6} - 1] \times 100\%$. (where AR is the aspect ratio of the elongated particle).

272

273 range of about 5-10 nm during DLS measurement for size distribution by intensity.⁶⁵ This
 274 artifact causes the hydrodynamic size determined by DLS to be smaller than the TEM
 275 determined core size, a result consistent with production of AuNPs by seed-mediated growth at
 276 100 °C.^{66, 67}

277 Gold nanoparticles display colors and LSPR bands in the visible spectral region that are
 278 dependent upon NP size and shape.^{11, 68, 69} The origin of the LSPR band is the coherent excitation
 279 of free conduction electrons due to polarization induced by the electric field of the incident light.
 280 A change in the absorbance or wavelength of the LSPR band provides a measure of particle size,
 281 shape, as well as aggregation state. UV-vis measurements were obtained to provide additional
 282 characterization of the nanoparticle properties. In Figure S6B, we provide both optical images
 283 and normalized UV-vis spectra for AuNPs of different sizes. For nanoparticle diameters between
 284 14 and 120 nm, the color exhibits a smooth transition from dark red to pink and ultimately to
 285 yellowish brown. As expected,⁷⁰ the LSPR wavelength is dependent on the nanoparticle size, as
 286 evinced by the increase of the maximum absorbance wavelength (λ_{max}) from 518 to 582 nm for
 287 nanoparticles of increasing size. This red shift is accompanied by the broadening of the LSPR
 288 band in the long wavelength region. This broadening may be due to an increase in

289 polydispersity,⁷¹ particle agglomeration,³¹ or a combination of both processes. Samples left at
 290 room temperature in the dark often agglomerated and precipitated, but could be easily re-
 291 suspended by shaking or sonication. Such storage exhibited no effect on nanoparticle stability.
 292

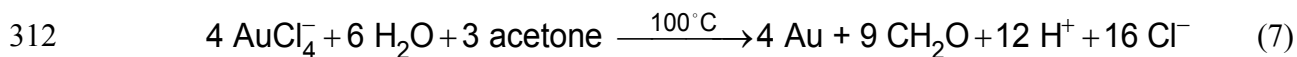


293
 294 Figure 2. TEM images of room temperature seed-mediated AuNPs of different sizes (aspect
 295 ratio): A) 24.0±6.1 nm (AR: 1.15±0.17), B) 37.1±4.6 nm (AR: 1.15±0.11), C) 46.0±4.6 nm (AR:
 296 1.34±0.14), D) 57.6±4.5 nm (AR: 1.14±0.06), E) 69.6±11.8 nm (AR: 1.13±0.07), F) 82.5±14.0
 297 nm (AR: 1.13±0.07), G) 92.4±11.4 nm (AR: 1.15±0.11), H) 100±11.4 nm (AR: 1.11±0.11), I)
 298 111.0±8.3 nm (AR: 1.11±0.09). Inset: histograms of diameters as determined by NIH ImageJ
 299 software.

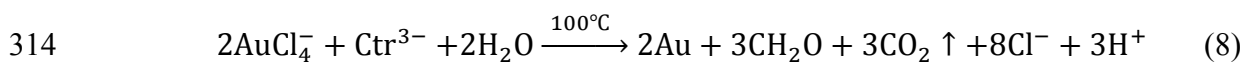
300
 301 **Monitoring seed-mediated AuNP growth process.** During AuNP synthesis, Ct^{3-} is oxidized
 302 to acetone dicarboxylate (ACDC^{2-} ; eqn. 5), a ligand that complexes Au^{III} , thus facilitating
 303 nanoparticle growth. Following nanoparticle nucleation, ACDC^{2-} is thought to be rapidly
 304 degraded to acetate at the synthesis temperature of $\approx 100\text{ }^\circ\text{C}$.⁹



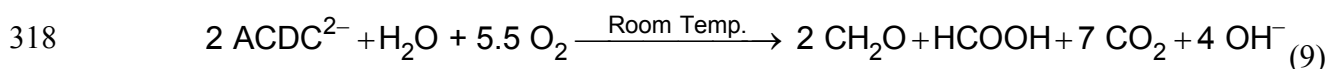
307 Past studies suggest that ACDC²⁻ or its degradation products take part in additional redox
 308 reactions when the Na₃Ctr /HAuCl₄ ratio is less than 1.5.⁶² Of particular relevance is a model
 309 developed based upon the kinetics of the AuNP formation which suggests that acetone or other
 310 carboxylate byproducts formed by the degradation of ACDC²⁻ (eqn. 6) reduce auric chloride and
 311 lead to its complete conversion to Au⁰ (eqn. 7).^{9,39}



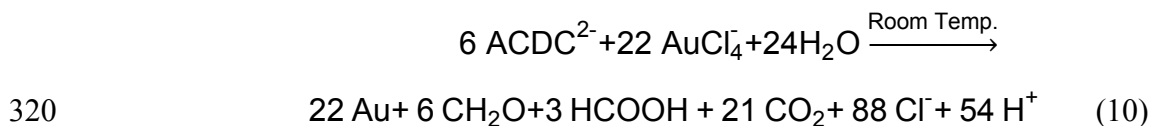
313 Summing up equations 5-7 and correcting for the reaction stoichiometry provides the following:



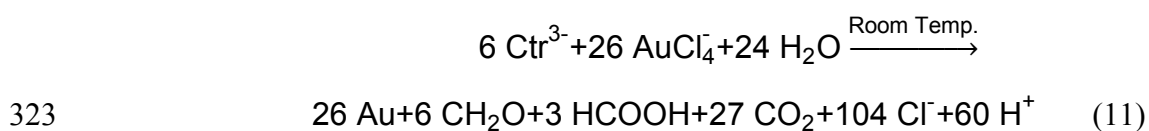
315 This model, however, does not consider the effects of temperature on ACDC²⁻ degradation. At
 316 room temperature it is known that ACDC²⁻ undergoes slow oxidation in the presence of
 317 oxygen.⁷²



319 We speculate the following similar reaction occurs preferentially in the presence of Au^{III}:

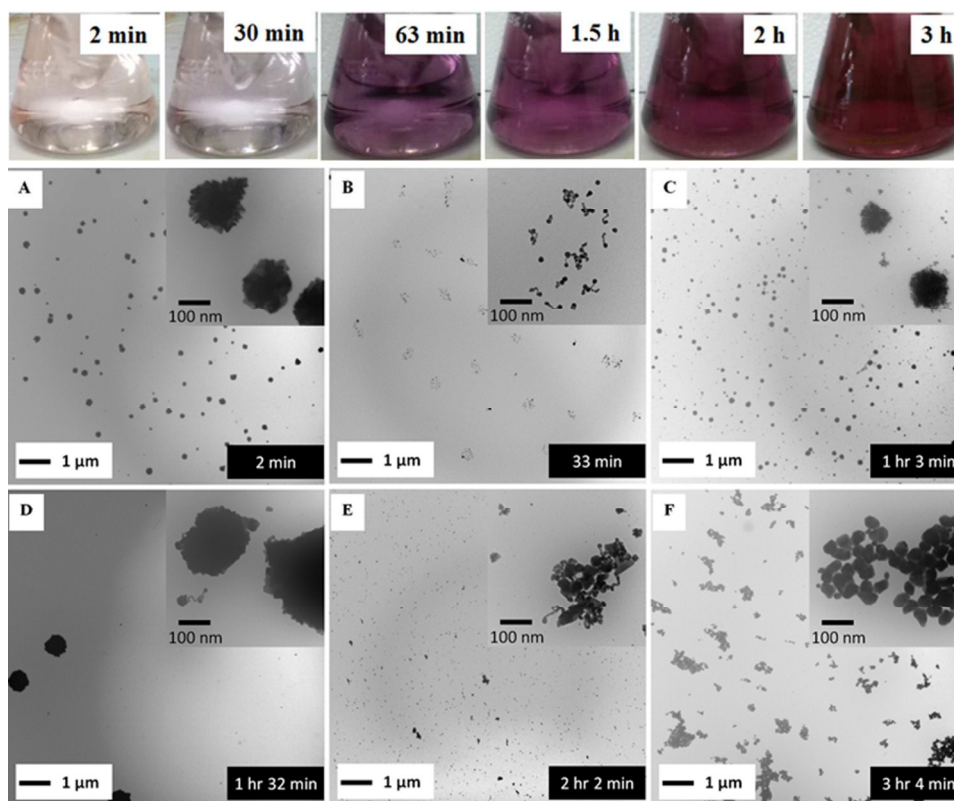


321 By summing up equations 5 and 10, the reaction stoichiometry in equation 11 indicates that 1
 322 mol of citrate can reduce > 4 mol of HAuCl₄.



324 We note that both Ctr³⁻ and ACDC²⁻ are carboxylates and that any byproducts of their oxidation,
 325 reduction, or degradation are likely to contain carboxylate groups.⁷³ Therefore, the carboxylate
 326 moiety is a likely means of interaction agent with the AuNP surface regardless of the exact
 327 species involved in AuNP capping.^{74,75}

328 As noted previously, room temperature reaction conditions slow the AuNP synthesis reaction,
 329 thus allowing for improved opportunities to characterize the seeded growth process. At room
 330 temperature, the suspension color changed very slowly, but followed a similar sequence as the
 331 traditional process at elevated temperature (i.e., from pale pink (seeds), to dark blue, to purple).
 332 Figure 3 shows typical TEM images for different growth times for seed mediated AuNPs
 333 prepared at a Na₃Ctr/HAuCl₄ ratio of 0.67 and a seed concentration of 5.35×10¹⁰ particles/mL

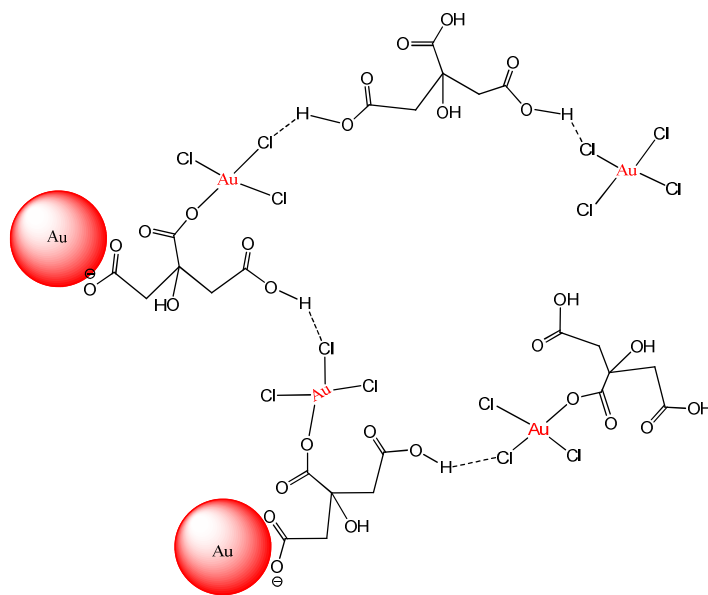


334
 335 Figure 3. Seed mediated growth for AuNPs (C) with mixed solution of HAuCl₄ (0.254 mM), Au
 336 seeds (5.35×10^{10} particle/ml), and Na₃Ctr (0.17 mM) at room temperature. TEM images of
 337 particles obtained at different growth times.
 338

339 (this corresponds to the ‘Type C’ AuNPs in Table 1). As shown in Figure S7, the UV absorption
 340 of Na₃Ctr decreases dramatically following Au^{III} addition, thus indicating its rapid coordination
 341 with Au^{III}. In this synthesis, Na₃Ctr facilitates coordination of Au^{III} ions around the AuNP seeds.
 342 This coordination involves fast ligand exchange between the carboxylates and chlorine ions
 343 within the AuCl_x(OH)_{4-x} complexes.³⁷

344 Previous studies suggest that the mode of interaction between Na₃Ctr and the AuNPs/Au ions
 345 is likely through a bidentate bridging mode or via unidentate or chelate modes.^{39, 76-78} As shown
 346 in Figure 3A, within 2 minutes of mixing the AuNP seeds with Na₃Ctr and HAuCl₄ we observed
 347 formation of large (> 100 nm) weakly associated clusters that consist of large numbers of AuNP
 348 seeds. These images are very similar to the large fluffy clusters observed by Chow and Zukoski
 349 in the early stage of AuNP synthesis at 60 °C.³⁵ Some of these crystallites may have formed
 350 following the drying of the suspension on the TEM grid. Nonetheless, this result suggests that
 351 carboxylates bound to the seed surface and present in the growth medium enhance the

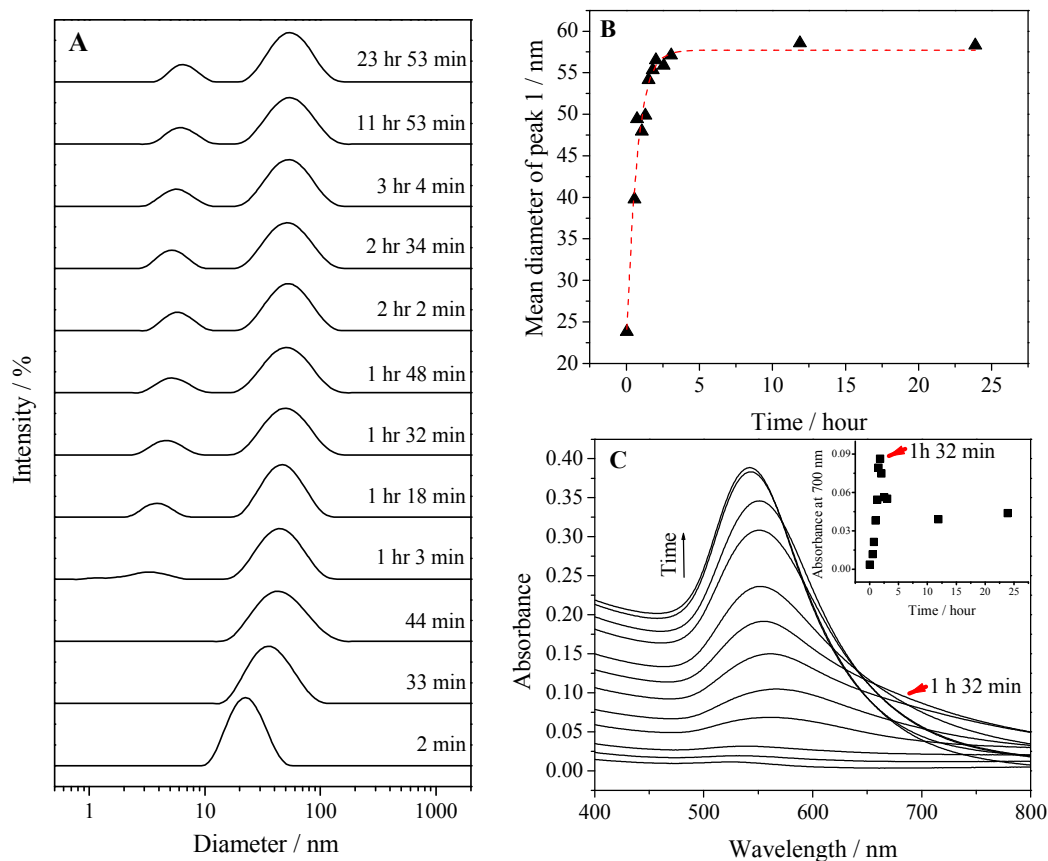
352 association between AuNP seeds and Au^{III} ions (Scheme 1). After 30 minutes the clusters are no
 353 longer observed and have broken apart due to the continued reaction between the carboxylates
 354 and Au^{III} and the suspension exhibits a light blue color. Figure 3B shows irregular gold
 355 nanowires together with aggregates at this growth stage, a result similar to the observations by Ji
 356 *et al.*³¹ and Pei *et al.*⁷⁹ for nanoparticles produced using Frens' method.⁸ After 1 hour, the gold
 357 nanowires form fluffy spherical networks (diameter \approx 100 nm; Figure 3C). In Figure 3C (inset),
 358 some irregular gold nanowires remain isolated from the larger network. As the reaction proceeds,
 359 however, the network continues to grow in size (Figure 3D). Similar trends in the AuNP
 360 synthesis progress at elevated temperatures have been reported by previous researchers.³⁵ After
 361 two hours, the fluffy network breaks apart into smaller segments (Figure 3E). Ultimately, as the
 362 color of the reaction suspension changes color to purple-red, spherical nanoparticles with
 363 diameter of 30-40 nm cleave off of the nanowires (Figure 3F). At the conclusion of the reaction,
 364 evinced by the unchanging particle diameter (Figure 4B) and LSPR peak (Figure 4C), the
 365 suspension attains a purple-red color and well-defined particles of 46 nm diameter are observed
 366 (Figure 2C).



367
 368 Scheme 1. Reactions among Au seeds, citrate and AuCl₄⁻ after initial mixing.

369
 370 Aliquots of the reaction suspensions were extracted and monitored by DLS and UV-Vis to
 371 further characterize the particle growth process depicted in Figure 3. Figure 4A illustrates the
 372 intensity weighted hydrodynamic size distributions determined by DLS at different growth

373 stages. In addition to the peak for the seeded particles in the region of 10-100 nm, a small size
374 distribution peak was detected after 1 hour of growth. This peak can be explained as a result of
375 the formation of non-spherical particles with one dimension elongated relative to the other. The
376 effects of rotational diffusion result in the appearance of a false peak in a size range of about 5-
377 10 nm during DLS measurement.⁶⁵ The presence of this peak is also consistent with the TEM
378 results in Figure 3C-F that show that there is a small proportion of particles with sizes less than
379 10 nm. The mean diameter of the major peak located between 10–100 nm increased dramatically
380 (Figure 4B) within an hour of Na₃Ctr addition and then stabilized at ≈57 nm after 3 hours. The
381 latter phenomenon agrees with the TEM result in Figure 3F, which shows that at this point the
382 reaction progress has neared completion of the “cleave” process. Interestingly, there is no
383 evidence in either Figure 4A or 4B of spherical networks with size in excess of 100 nm, which
384 suggests that the large networks may have formed during TEM sample preparation. Capillary
385 drying forces are well known to result in enhanced nanoparticle association following drop
386 drying.⁸⁰ The association between solution phase Au^{III} and the AuNPs is reflected in the
387 absorption spectra in Figure 4C. There was a broad absorption at wavelengths > 600 nm that
388 increased in magnitude as time increased from t=2 min to t=92 min. This phase of the particle
389 size evolution corresponds to Figure 3A-D, during which the AuNPs form fluffy networks. The
390 broadening of the LSPR peak in the region >600 nm (Figure 4C) and the increased absorbance
391 at 700 nm (Figure 4C inset) corresponds to these fluffy networks. After 92 minutes, a sharp red-
392 shift in the LSPR peak was observed (Figure 4C), which has been referred to as “turnover” in the
393 literature⁸¹. The “turnover” point at t=92 min supports the structure/size change from Figure 3D
394 to 3E, during which the fluffy networked structure gave way to discrete AuNPs, which also
395 corresponds to the decreased absorbance at 700 nm (Figure 4C inset).



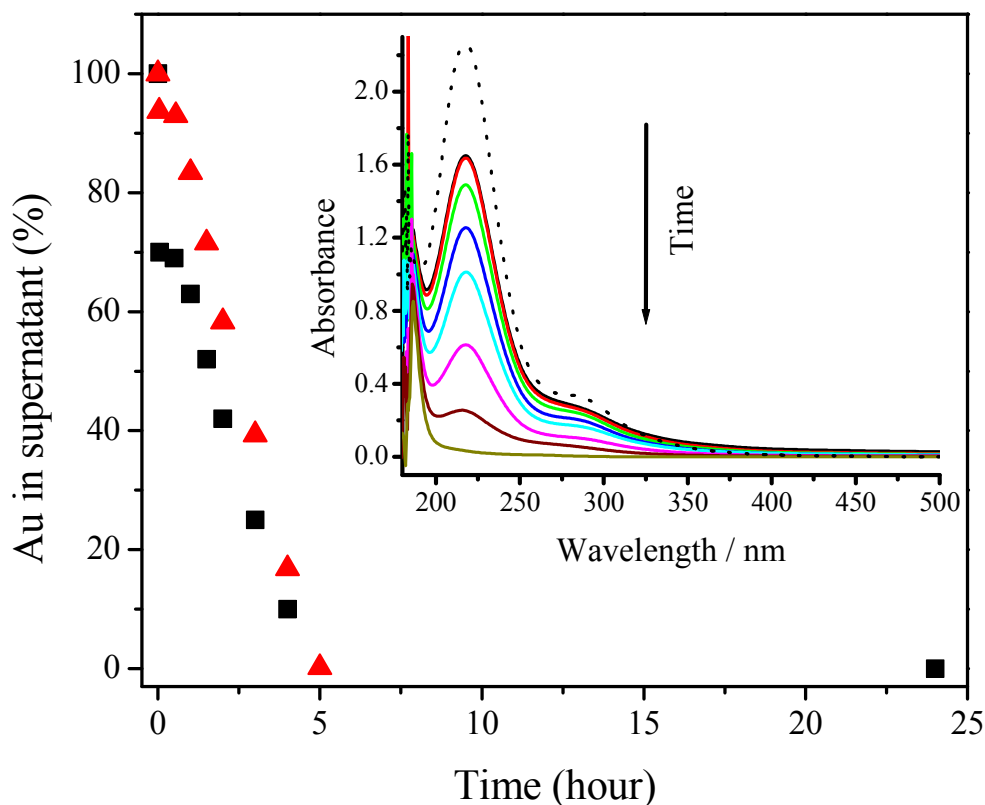
396

397 Figure 4. (A) Size distribution by intensity, (B) mean diameter of peak 1 (located in the range of
 398 10 – 100 nm in A) and (C) UV-vis absorption spectra obtained at different time stages of seed
 399 growth synthesis of AuNPs.

400

401 Reaction supernatants separated by centrifugation at each reaction time were analyzed by
 402 UV-vis spectroscopy and ICP-MS. As shown in Figure 5, the absorbance at ≈ 218 nm, which
 403 corresponds to unreacted Au^{III} ,⁸² decreases rapidly after the initial mixing of the reagents,
 404 stabilizes for approximately 30 minutes, and then decreases linearly with time. Compared to the
 405 initial Au^{III} peak intensity at 218 nm, $\approx 30\%$ of added Au^{III} was reduced after the initial mixing of
 406 the reagents. In contrast, over this initial period, $\approx 93\%$ of total Au was detected by ICP-MS in
 407 the reaction supernatant, thus suggesting the presence of an intermediate reduced product of Au^{III}
 408 (i.e., Au^{I}) or very small AuNPs. Such a result is consistent with rapid coordination between the
 409 carboxylates and Au^{III} and association of these complexes with the Au seeds (i.e., the clusters of
 410 seeds and Au^{III} shown in Figure 3A). The Au^{III} concentration was then stable for next 30 minutes.
 411 Such a result suggests that the initial oxidation-reduction reaction only takes place in the clusters
 412 shown in Figure 3A and Scheme 1, which is consistent with the change from Figure 3A to 3B.

413 After the initial 30 minutes of reaction, both the concentration of Au^{III} and total Au in the
414 supernatant began to decrease linearly and a total reaction time of ≈ 5 hours was observed. We
415 used UV-vis spectroscopy to verify that the AuNP growth reaction proceeded according to
416 equation 11. A mixture of HCl and NaCl with relative concentrations based upon the
417 stoichiometry of equation 11 was prepared to compare with the UV absorbance of the
418 supernatant of the reaction solution after 5 hours reaction. The near perfect match of the spectra
419 shown in Figure S8 provides evidence that the stoichiometry of the room temperature seed
420 mediated growth process is reasonably described by equation 11. Moreover, no residual gold
421 chloride ion was detected in the UV-vis spectrum of the supernatant. As has been previously
422 reported,³¹ residual gold exhibits a peak at 218-314 nm in the UV-vis spectra. The absence of
423 this peak in the final UV-vis spectra suggests that there was no residual gold ion. For this reason
424 a 100% reaction yield was assumed, and verified by the ICP-MS results in Figure 5 To the best
425 of our knowledge this is the first time a reaction stoichiometry has been developed for room-
426 temperature seed-mediated AuNP synthesis.
427

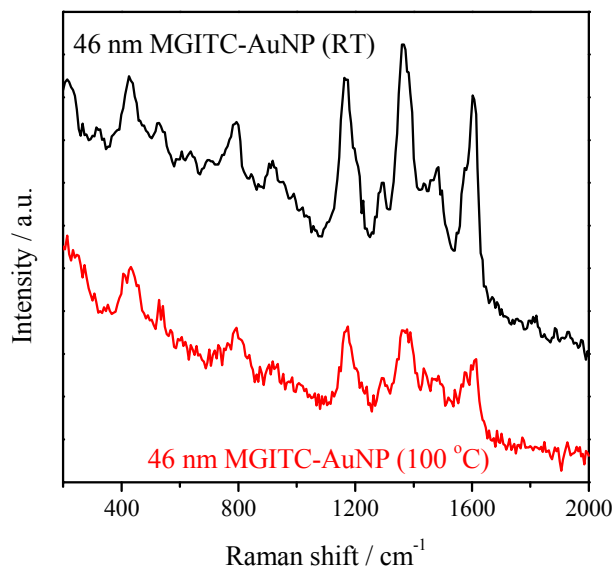


428

429 Figure 5. Time-dependent Au^{III} and Au levels in supernatant as determined by UV-vis (squares)
430 and ICP-MS (triangles). Inset: corresponding UV absorption spectra. Dash black line is the
431 spectrum of the initial Au^{III} solution. Prior to the UV-vis measurement, all AuNP suspensions
432 were diluted 2× with deionized water.
433

434 ***Evaluation of room temperature seeded AuNPs.*** The as-prepared AuNPs exhibit exceptional
435 colloidal stability and can be stored at room temperature over several months in spite of their
436 slow agglomeration. The nanoparticles could be easily re-suspended by shaking or sonication.
437 This result suggests these particles can be favorably employed for SERS applications. Figure 6
438 compares the surface Raman enhancement of MGITC adsorbed on seed mediated 46 nm AuNPs
439 produced at room temperature with those produced at 100 °C (Figure S9, Supporting
440 Information). Importantly, the AuNPs prepared at room temperature exhibit a 2× greater Raman
441 enhancement than AuNPs prepared at 100 °C. We attribute this enhancement to the greater
442 surface roughness of the room temperature AuNPs.⁸³

443 Particles with edges, corners, and branches (e.g., nanorods, nanostars) are quasi-stable at low
444 temperature, but transform into more thermodynamically stable shapes (i.e., spheres) if sufficient
445 thermal energy is provided for atomic reorganization. As shown by TEM imaging (Figure S9),
446 the particles prepared at room temperature exhibit more edges and corners than comparable
447 particles prepared at 100 °C thus suggesting the lower synthesis temperature enhances their
448 formation. Because the concentration and volume of AuNPs was constant, the surface area of the
449 particles produced at room temperature will be larger than those synthesized at 100°C, thus
450 leading to an enhanced surface roughness and thus higher SERS enhancement relative to AuNPs
451 prepared at 100 °C.



452 Figure 6. SERS spectra of MGITC (20 nM) adsorbed on room temperature and 100 °C seed
 453 mediated AuNPs under 633 nm excitation. MGITC-AuNPs were prepared by quickly adding
 454 $\approx 1.5 \mu\text{L}$ of 14 μM MGITC solution to 1 mL AuNP suspension (5.4×10^{10} particle/mL).
 455
 456

457 **Comparative LCA.** The cumulative energy demands
 458 (CED) of the AuNP synthesis methods determined by the
 459 LCA models are presented in Table 2. The results show
 460 that despite the longer reaction time, AuNP synthesis at
 461 room temperature has lower CED than synthesis under
 462 boiling conditions. The trend of the other impacts across
 463 different impact categories matches that of the CED
 464 (Figure S10, Supporting Information). This result is
 465 expected as CED has been shown to correlate well to
 466 other environmental impact methods (e.g., EcoIndicator,
 467 EcoScarcity, etc.).⁸⁴ This observation is understandable
 468 because the use of fossil fuels (included in CED) is a
 469 dominant driver of many environmental impacts.⁸⁵

470
 471 Uncertainty analysis shows that the differences in the
 472 environmental impacts for AuNP synthesis at room
 473 temperature and under boiling conditions are statistically

Table 2. Cumulative energy demand (CED) for AuNP synthesis at room temperature vs. boiling conditions. The CEDs for AuNP syntheses at room temperature and under boiling conditions are 1.25 MJ and 1.54 MJ respectively.

Synthesis at room temperature		
Material and energy inputs	Cumulative energy demand (MJ)	% contribution
Chloroauric acid	4.07×10^{-1}	32.59%
Deionized water	8.31×10^{-3}	0.67%
Aqua regia	5.67×10^{-2}	4.54%
AuNP 'seeds'	1.60×10^{-2}	1.28%
Sodium hydroxide	5.27×10^{-7}	$4.22 \times 10^{-5}\%$
Trisodium citrate	5.12×10^{-6}	$4.10 \times 10^{-4}\%$
Stirring	7.61×10^{-1}	60.93%
Total	1.25×10^0	100.00%

Synthesis under boiling conditions		
Material and energy inputs	Cumulative energy demand (MJ)	% contribution
Chloroauric acid	4.07×10^{-1}	26.48%
DI water	8.31×10^{-3}	0.54%
Tap water	1.67×10^{-4}	0.01%
Aqua regia	5.67×10^{-2}	3.69%
AuNP 'seeds'	1.60×10^{-2}	1.04%
Sodium hydroxide	5.27×10^{-7}	$3.43 \times 10^{-5}\%$
Trisodium citrate	5.12×10^{-6}	$3.33 \times 10^{-4}\%$
Heating	9.73×10^{-1}	63.29%
Stirring	7.61×10^{-2}	4.95%
Total	1.54×10^0	100.00%

474 significant (Figure S11). Although laboratory-scale room temperature synthesis does seem to
475 reduce the energy footprint of AuNP synthesis (compared to the conventional approach at higher
476 temperatures), further studies on scale-up scenarios are recommended, since the environmental
477 footprints are likely to be influenced by yield, energy efficiencies and the available energy
478 sources and fuel-mixes.^{86, 87} Conventional scale-up of boilers and generators has been shown to
479 follow a power law relationship.^{88, 89} However, similar relationships for scaling up have not been
480 established for nanoparticle synthesis. Longer reaction times in pilot-scale and commercial-scale
481 setups will involve additional energy demands (e.g., lighting, heat ventilation, air-conditioning
482 etc.) that should also be considered in scale up scenarios. The role of regional variability in the
483 energy and water footprints should also be factored into future decisions about nanomaterials
484 industry siting and resource allocation.

485

486 CONCLUSIONS

487 A simple room temperature seed mediated preparation route for AuNPs has been
488 demonstrated. Tunability of the AuNP diameter was achieved by simply varying the number
489 concentration of seeds under mild environmental conditions. Such a result shows a promising
490 colorimetric assay using the size-dependent optical property. The continuous surface plasmon
491 oscillations associated with this broad spectral feature gives them broad selection in the future
492 SERS applications. Our reported AuNP synthesis approach helps decrease the rate of AuNP
493 growth due to the milder (room temperature) conditions, thus providing increased opportunities
494 to study a very complicated reaction mechanism. Moreover, this method shows significant
495 reductions in the cradle-to-gate life cycle impacts compared to the previously reported methods
496 that employed boiling conditions.

497

498 ACKNOWLEDGMENT

499 This work was supported by grants from the Virginia Tech Graduate School (Sustainable
500 Nanotechnology Interdisciplinary Graduate Education Program), the Virginia Tech Institute of
501 Critical Technology and Applied Science (ICTAS), and NSF Award CBET-1133746.

502

503 REFERENCES

504

- 505 1. Kushnir, D.; Sandén, B. A., Multi-Level Energy Analysis of Emerging Technologies: A
506 Case Study in New Materials for Lithium Ion Batteries. *Journal of Cleaner Production* **2011**, *19*,
507 (13), 1405-1416.
- 508 2. Kushnir, D.; Sandén, B. A., Energy Requirements of Carbon Nanoparticle Production.
509 *Journal of Industrial Ecology* **2008**, *12*, (3), 360-375.
- 510 3. Murphy, C. J., Sustainability as an emerging design criterion in nanoparticle synthesis
511 and applications. *J. Mater. Chem.* **2008**, *18*, (19), 2173-2176.
- 512 4. Grzelczak, M.; Pérez-Juste, J.; Mulvaney, P.; Liz-Marzán, L. M., Shape control in gold
513 nanoparticle synthesis. *Chemical Society Reviews* **2008**, *37*, (9), 1783-1791.
- 514 5. Dahl, J. A.; Maddux, B. L. S.; Hutchison, J. E., Toward Greener Nanosynthesis.
515 *Chemical Reviews* **2007**, *107*, (6), 2228-2269.
- 516 6. Hutchison, J. E., Greener Nanoscience: A Proactive Approach to Advancing Applications
517 and Reducing Implications of Nanotechnology. *ACS Nano* **2008**, *2*, (3), 395-402.
- 518 7. McKenzie, L. C.; Hutchison, J. E., Green nanoscience. *Chimica oggi* **2004**, *22*, (9), 30-33.
- 519 8. Frens, G., Controlled Nucleation for the Regulation of the Particle Size in Monodisperse
520 Gold Suspensions. *Nature* **1973**, *241*, (105), 20-22.
- 521 9. Turkevich, J.; Stevenson, P. C.; Hillier, J., The nucleation and growth processes in the
522 synthesis of colloidal gold. *Discuss. Faraday Soc.* **1951**, No. 11, 55-75.
- 523 10. Kogan, M. J.; Bastus, N. G.; Amigo, R.; Grillo-Bosch, D.; Araya, E.; Turiel, A.; Labarta,
524 A.; Giralt, E.; Puentes, V. F., Nanoparticle-Mediated Local and Remote Manipulation of Protein
525 Aggregation. *Nano Letters* **2006**, *6*, (1), 110-115.
- 526 11. Daniel, M.-C.; Astruc, D., Gold Nanoparticles: Assembly, Supramolecular Chemistry,
527 Quantum-Size-Related Properties, and Applications toward Biology, Catalysis, and
528 Nanotechnology. *Chemical Reviews (Washington, DC, United States)* **2004**, *104*, (1), 293-346.
- 529 12. Bastus, N. G.; Sanchez-Tillo, E.; Pujals, S.; Farrera, C.; Lopez, C.; Giralt, E.; Celada, A.;
530 Lloberas, J.; Puentes, V., Homogeneous Conjugation of Peptides onto Gold Nanoparticles
531 Enhances Macrophage Response. *ACS Nano* **2009**, *3*, (6), 1335-1344.
- 532 13. Connor, E. E.; Mwamuka, J.; Gole, A.; Murphy, C. J.; Wyatt, M. D., Gold nanoparticles
533 are taken up by human cells but do not cause acute cytotoxicity. *Small* **2005**, *1*, (3), 325-327.
- 534 14. Chen, Y.-S.; Hung, Y.-C.; Liao, I.; Huang, G. S., Assessment of the in vivo toxicity of
535 gold nanoparticles. *Nanoscale Research Letters* **2009**, *4*, (8), 858-864.
- 536 15. Hauck, T. S.; Ghazani, A. A.; Chan, W. C. W., Assessing the effect of surface chemistry
537 on gold nanorod uptake, toxicity, and gene expression in mammalian cells. *Small* **2008**, *4*, (1),
538 153-159.
- 539 16. Brown, S. D.; Nativo, P.; Smith, J.-A.; Stirling, D.; Edwards, P. R.; Venugopal, B.; Flint,
540 D. J.; Plumb, J. A.; Graham, D.; Wheate, N. J., Gold Nanoparticles for the Improved Anticancer
541 Drug Delivery of the Active Component of Oxaliplatin. *Journal of the American Chemical*
542 *Society* **2010**, *132*, (13), 4678-4684.
- 543 17. Bhattacharyya, S.; Bhattacharya, R.; Curley, S.; McNiven, M. A.; Mukherjee, P.,
544 Nanoconjugation modulates the trafficking and mechanism of antibody induced receptor
545 endocytosis. *Proceedings of the National Academy of Sciences of the United States of America*
546 **2010**, *107*, (33), 14541-14546, S14541/1-S14541/8.
- 547 18. Tkachenko, A. G.; Xie, H.; Coleman, D.; Glomm, W.; Ryan, J.; Anderson, M. F.;
548 Franzen, S.; Feldheim, D. L., Multifunctional gold nanoparticle-peptide complexes for nuclear
549 targeting. *Journal of the American Chemical Society* **2003**, *125*, (16), 4700-4701.

- 550 19. Kang, B.; Mackey, M. A.; El-Sayed, M. A., Nuclear Targeting of Gold Nanoparticles in
551 Cancer Cells Induces DNA Damage, Causing Cytokinesis Arrest and Apoptosis. *Journal of the*
552 *American Chemical Society* **2010**, *132*, (5), 1517-1519.
- 553 20. Oh, E.-K.; Delehanty, J. B.; Sapsford, K. E.; Susumu, K.; Goswami, R.; Blanco-Canosa,
554 J. B.; Dawson, P. E.; Granek, J.; Shoff, M.; Zhang, Q.; Goering, P. L.; Huston, A.; Medintz, I. L.,
555 Cellular Uptake and Fate of PEGylated Gold Nanoparticles Is Dependent on Both Cell-
556 Penetration Peptides and Particle Size. *ACS Nano* **2011**, *5*, (8), 6434-6448.
- 557 21. Paciotti, G. F.; Kingston, D. G. I.; Tamarkin, L., Colloidal gold nanoparticles: a novel
558 nanoparticle platform for developing multifunctional tumor-targeted drug delivery vectors. *Drug*
559 *Development Research* **2006**, *67*, (1), 47-54.
- 560 22. Upadhyayula, V. K. K., Functionalized gold nanoparticle supported sensory mechanisms
561 applied in detection of chemical and biological threat agents: A review. *Analytica Chimica Acta*
562 **2012**, *715*, 1-18.
- 563 23. Wang, J., Nanomaterial-based amplified transduction of biomolecular interactions. *Small*
564 **2005**, *1*, (11), 1036-1043.
- 565 24. He, P.; Shen, L.; Liu, R.; Luo, Z.; Li, Z., Direct Detection of N₂-Agonists by Use of Gold
566 Nanoparticle-Based Colorimetric Assays. *Analytical Chemistry (Washington, DC, United States)*
567 **2012**, *83*, (18), 6988-6995.
- 568 25. Pellegrino, T.; Kudera, S.; Liedl, T.; Javier, A. M.; Manna, L.; Parak, W. J., On the
569 development of colloidal nanoparticles towards multifunctional structures and their possible use
570 for biological applications. *Small* **2005**, *1*, (1), 48-63.
- 571 26. Scampicchio, M.; Wang, J.; Blasco, A. J.; Arribas, A. S.; Mannino, S.; Escarpa, A.,
572 Nanoparticle-Based Assays of Antioxidant Activity. *Analytical Chemistry* **2006**, *78*, (6), 2060-
573 2063.
- 574 27. Willner, I.; Baron, R.; Willner, B., Growing metal nanoparticles by enzymes. *Advanced*
575 *Materials (Weinheim, Germany)* **2006**, *18*, (9), 1109-1120.
- 576 28. Burda, C.; Chen, X.; Narayanan, R.; El-Sayed, M. A., Chemistry and Properties of
577 Nanocrystals of Different Shapes. *Chemical Reviews (Washington, DC, United States)* **2005**, *105*,
578 (4), 1025-1102.
- 579 29. Nikoobakht, B.; El-Sayed, M. A., Preparation and growth mechanism of gold nanorods
580 (NRs) using seed-mediated growth method. *Chemistry of Materials* **2003**, *15*, (10), 1957-1962.
- 581 30. Murphy, C. J.; Jana, N. R., Controlling the aspect ratio of inorganic nanorods and
582 nanowires. *Advanced Materials* **2002**, *14*, (1), 80-82.
- 583 31. Ji, X.; Song, X.; Li, J.; Bai, Y.; Yang, W.; Peng, X., Size Control of Gold Nanocrystals in
584 Citrate Reduction: The Third Role of Citrate. *Journal of the American Chemical Society* **2007**,
585 *129*, (45), 13939-13948.
- 586 32. Jana, N. R.; Gearheart, L.; Murphy, C. J., Seeding growth for size control of 5-40 nm
587 diameter gold nanoparticles. *Langmuir* **2001**, *17*, (22), 6782-6786.
- 588 33. Kimling, J.; Maier, M.; Okenve, B.; Kotaidis, V.; Ballot, H.; Plech, A., Turkevich
589 Method for Gold Nanoparticle Synthesis Revisited. *J. Phys. Chem. B* **2006**, *110*, (32), 15700-
590 15707.
- 591 34. Frens, G., Controlled nucleation for the regulation of the particle size in monodisperse
592 gold suspensions. *Nature (London), Physical Science* **1973**, *241*, (105), 20-2.
- 593 35. Chow, M. K.; Zukoski, C. F., Gold sol formation mechanisms: role of colloidal stability.
594 *Journal of Colloid and Interface Science* **1994**, *165*, (1), 97-109.

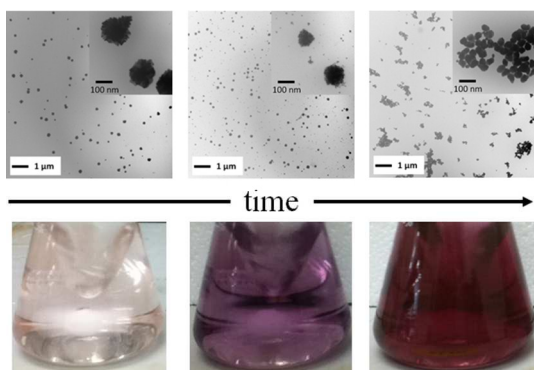
- 595 36. Turkevich, J.; Stevenson, P. C.; Hillier, J., The formation of colloidal gold. *Journal of*
596 *Physical Chemistry* **1953**, *57*, 670-3.
- 597 37. Ojea-Jimenez, I.; Romero, F. M.; Bastus, N. G.; Puntès, V., Small Gold Nanoparticles
598 Synthesized with Sodium Citrate and Heavy Water: Insights into the Reaction Mechanism.
599 *Journal of Physical Chemistry C* **2010**, *114*, (4), 1800-1804.
- 600 38. Henglein, A.; Giersig, M., Formation of colloidal silver nanoparticles. Capping action of
601 citrate. *J. Phys. Chem. B* **1999**, *103*, (44), 9533-9539.
- 602 39. Kumar, S.; Gandhi, K. S.; Kumar, R., Modeling of formation of gold nanoparticles by
603 citrate method. *Industrial & Engineering Chemistry Research* **2007**, *46*, (10), 3128-3136.
- 604 40. Sau, T. K.; Murphy, C. J., Room Temperature, High-Yield Synthesis of Multiple Shapes
605 of Gold Nanoparticles in Aqueous Solution. *Journal of the American Chemical Society* **2004**,
606 *126*, (28), 8648-8649.
- 607 41. Nadagouda, M. N.; Varma, R. S., Green synthesis of silver and palladium nanoparticles
608 at room temperature using coffee and tea extract. *Green Chemistry* **2008**, *10*, (8), 859-862.
- 609 42. Perrault, S. D.; Chan, W. C. W., Synthesis and Surface Modification of Highly
610 Monodispersed, Spherical Gold Nanoparticles of 50–200 nm. *Journal of the American Chemical*
611 *Society* **2009**, *131*, (47), 17042-17043.
- 612 43. Ziegler, C.; Eychmüller, A., Seeded Growth Synthesis of Uniform Gold Nanoparticles
613 with Diameters of 15–300 nm. *The Journal of Physical Chemistry C* **2011**, *115*, (11), 4502-4506.
- 614 44. Anastas, P. T.; Warner, J. C., *Green chemistry: theory and practice*. Oxford University
615 Press, USA: 2000.
- 616 45. Pati, P.; McGinnis, S.; Vikesland, P. J., Life Cycle Assessment of “Green” Nanoparticle
617 Synthesis Methods. *Environmental Engineering Science* **2014**.
- 618 46. Walser, T.; Demou, E.; Lang, D. J.; Hellweg, S., Prospective Environmental Life Cycle
619 Assessment of Nanosilver T-Shirts. *Environmental Science & Technology* **2011**, *45*, (10), 4570-
620 4578.
- 621 47. Bauer, C.; Buchgeister, J.; Hischer, R.; Poganietz, W. R.; Schebek, L.; Warsen, J.,
622 Towards a Framework for Life Cycle Thinking in the Assessment of Nanotechnology. *Journal of*
623 *Cleaner Production* **2008**, *16*, (8–9), 910-926.
- 624 48. Kim, H. C.; Fthenakis, V., Life Cycle Energy and Climate Change Implications of
625 Nanotechnologies. *Journal of Industrial Ecology* **2013**, *17*, (4), 528-541.
- 626 49. Li, Q.; McGinnis, S.; Sydnor, C.; Wong, A.; Renneckar, S., Nanocellulose Life Cycle
627 Assessment. *ACS Sustainable Chem. Eng.* **2013**, *1*, (8), 919-928.
- 628 50. Upadhyayula, V. K. K.; Meyer, D. E.; Curran, M. A.; Gonzalez, M. A., Evaluating the
629 Environmental Impacts of a Nano-Enhanced Field Emission Display Using Life Cycle
630 Assessment: A Screening-Level Study. *Environmental Science & Technology* **2013**.
- 631 51. Chen, H.; Kou, X.; Yang, Z.; Ni, W.; Wang, J., Shape- and Size-Dependent Refractive
632 Index Sensitivity of Gold Nanoparticles. *Langmuir* **2008**, *24*, (10), 5233-5237.
- 633 52. Liu, X.; Atwater, M.; Wang, J.; Huo, Q., Extinction coefficient of gold nanoparticles with
634 different sizes and different capping ligands. *Colloids and Surfaces, B: Biointerfaces* **2007**, *58*,
635 (1), 3-7.
- 636 53. Haiss, W.; Thanh, N. T. K.; Aveyard, J.; Fernig, D. G., Determination of size and
637 concentration of gold nanoparticles from UV-Vis spectra. *Analytical Chemistry* **2007**, *79*, (11),
638 4215-4221.

- 639 54. Bastus, N. G.; Comenge, J.; Puentes, V., Kinetically Controlled Seeded Growth Synthesis
640 of Citrate-Stabilized Gold Nanoparticles of up to 200 nm: Size Focusing versus Ostwald
641 Ripening. *Langmuir* **2011**, *27*, (17), 11098-11105.
- 642 55. Guinée, J. B.; Heijungs, R.; Huppel, G.; Zamagni, A.; Masoni, P.; Buonamici, R.; Ekvall,
643 T.; Rydberg, T., Life Cycle Assessment: Past, Present, and Future†. *Environmental Science &*
644 *Technology* **2011**, *45*, (1), 90-96.
- 645 56. Frischknecht, R.; Jungbluth, N.; Althaus, H.-J.; Doka, G.; Dones, R.; Heck, T.; Hellweg,
646 S.; Hischer, R.; Nemecek, T.; Rebitzer, G., The ecoinvent database: Overview and
647 methodological framework (7 pp). *The International Journal of Life Cycle Assessment* **2005**, *10*,
648 (1), 3-9.
- 649 57. Pati, P.; McGinnis, S.; Vikesland, P. J., Life Cycle Assessment of "Green" Nanoparticle
650 Synthesis Methods. *Environ. Eng. Sci.* **2014**, *31*, (7), 410-420.
- 651 58. Frischknecht, R.; Jungbluth, N.; Althaus, H. J.; Bauer, C.; Doka, G.; Dones, R.; Hischer,
652 R.; Hellweg, S.; Humbert, S.; Köllner, T. *Implementation of life cycle impact assessment*
653 *methods*; 3; EcoInvent Report: 2007, 2007.
- 654 59. Machesky, M. L.; Andrade, W. O.; Rose, A. W., Adsorption of gold(III)-chloride and
655 gold(I)-thiosulfate anions by goethite. *Geochimica et Cosmochimica Acta* **1991**, *55*, (3), 769-76.
- 656 60. Goia, D. V.; Matijevic, E., Tailoring the particle size of monodispersed colloidal gold.
657 *Colloids and Surfaces, A: Physicochemical and Engineering Aspects* **1999**, *146*, (1-3), 139-152.
- 658 61. Wang, S.; Qian, K.; Bi, X.; Huang, W., Influence of Speciation of Aqueous HAuCl₄ on
659 the Synthesis, Structure, and Property of Au Colloids. *Journal of Physical Chemistry C* **2009**,
660 *113*, (16), 6505-6510.
- 661 62. Brown, K. R.; Walter, D. G.; Natan, M. J., Seeding of colloidal Au nanoparticle solutions.
662 2. Improved control of particle size and shape. *Chemistry of Materials* **2000**, *12*, (2), 306-313.
- 663 63. Brown, K. R.; Walter, D. G.; Natan, M. J., Seeding of colloidal Au nanoparticle solutions.
664 2. Improved control of particle size and shape. *Chemistry of Materials* **2000**, *12*, (2), 306-313.
- 665 64. Thomas, J. C., The determination of log normal particle size distributions by dynamic
666 light scattering. *Journal of Colloid and Interface Science* **1987**, *117*, (1), 187-92.
- 667 65. Khlebtsov, B. N.; Khlebtsov, N. G., On the measurement of gold nanoparticle sizes by
668 the dynamic light scattering method. *Colloid Journal* **2011**, *73*, (1), 118-127.
- 669 66. Hull, M. S.; Chaurand, P.; Rose, J.; Auffan, M.; Bottero, J.-Y.; Jones, J. C.; Schultz, I. R.;
670 Vikesland, P. J., Filter-Feeding Bivalves Store and Biodeposit Colloidally Stable Gold
671 Nanoparticles. *Environmental Science and Technology* **2011**, *45*, (15), 6592-6599.
- 672 67. Leng, W.; Vikesland, P. J., MGITC Facilitated Formation of AuNP Multimers. *Langmuir*
673 **2014**, *30*, (28), 8342-8349.
- 674 68. Liz-Marzan, L. M., Tailoring Surface Plasmons through the Morphology and Assembly
675 of Metal Nanoparticles. *Langmuir* **2006**, *22*, (1), 32-41.
- 676 69. Murphy, C. J.; San, T. K.; Gole, A. M.; Orendorff, C. J.; Gao, J. X.; Gou, L.; Hunyadi, S.
677 E.; Li, T., Anisotropic metal nanoparticles: Synthesis, assembly, and optical applications.
678 *Journal of Physical Chemistry B* **2005**, *109*, (29), 13857-13870.
- 679 70. Kelly, K. L.; Coronado, E.; Zhao, L. L.; Schatz, G. C., The Optical Properties of Metal
680 Nanoparticles: The Influence of Size, Shape, and Dielectric Environment. *J. Phys. Chem. B* **2003**,
681 *107*, (3), 668-677.
- 682 71. Wilcoxon, J. P.; Martin, J. E.; Provencio, P., Optical properties of gold and silver
683 nanoclusters investigated by liquid chromatography. *The Journal of Chemical Physics* **2001**, *115*,
684 (2), 998-1008.

- 685 72. Kuyper, A. C., Oxidation of citric acid. *Journal of the American Chemical Society* **1933**,
686 55, 1722-7.
- 687 73. Munro, C. H.; Smith, W. E.; Garner, M.; Clarkson, J.; White, P. C., Characterization of
688 the Surface of a Citrate-Reduced Colloid Optimized for Use as a Substrate for Surface-Enhanced
689 Resonance Raman Scattering. *Langmuir* **1995**, *11*, (10), 3712-3720.
- 690 74. Tang, B.; Tao, J.; Xu, S.; Wang, J.; Hurren, C.; Xu, W.; Sun, L.; Wang, X., Using
691 hydroxy carboxylate to synthesize gold nanoparticles in heating and photochemical reactions and
692 their application in textile coloration. *Chemical Engineering Journal (Amsterdam, Netherlands)*
693 **2011**, *172*, (1), 601-607.
- 694 75. Iosin, M.; Baldeck, P.; Astilean, S., Study of tryptophan assisted synthesis of gold
695 nanoparticles by combining UV-Vis, fluorescence, and SERS spectroscopy. *Journal of*
696 *Nanoparticle Research* **2010**, *12*, (8), 2843-2849.
- 697 76. Turkevich, J., Colloidal gold. Part I. Historical and preparative aspects, morphology and
698 structure. *Gold Bulletin (Geneva)* **1985**, *18*, (3), 86-91.
- 699 77. Turkevich, J., Colloidal gold. Part II. Color, coagulation, adhesion, alloying and catalytic
700 properties. *Gold Bulletin (Geneva)* **1985**, *18*, (4), 125-31.
- 701 78. Hull, J. M.; Provorse, M. R.; Aikens, C. M., Formylxoyl Radical-Gold Nanoparticle
702 Binding: A Theoretical Study. *Journal of Physical Chemistry A* **2012**, *116*, (22), 5445-5452.
- 703 79. Pei, L.; Mori, K.; Adachi, M., Formation Process of Two-Dimensional Networked Gold
704 Nanowires by Citrate Reduction of AuCl₄⁻ and the Shape Stabilization. *Langmuir* **2004**, *20*, (18),
705 7837-7843.
- 706 80. Chang, X.; Vikesland, P. J., Uncontrolled Variability in the Extinction Spectra of C60
707 Nanoparticle Suspensions. *Langmuir* **2013**, *29*, (31), 9685-9693.
- 708 81. Peng, S.; McMahon, J. M.; Schatz, G. C.; Gray, S. K.; Sun, Y., Reversing the size-
709 dependence of surface plasmon resonances. *Proceedings of the National Academy of Sciences of*
710 *the United States of America* **2010**, *107*, (33), 14530-14534.
- 711 82. Peck, J. A.; Tait, C. D.; Swanson, B. I.; Brown Jr, G. E., Speciation of aqueous gold(III)
712 chlorides from ultraviolet/visible absorption and Raman/resonance Raman spectroscopies.
713 *Geochimica et Cosmochimica Acta* **1991**, *55*, (3), 671-676.
- 714 83. Talley, C. E.; Jackson, J. B.; Oubre, C.; Grady, N. K.; Hollars, C. W.; Lane, S. M.; Huser,
715 T. R.; Nordlander, P.; Halas, N. J., Surface-Enhanced Raman Scattering from Individual Au
716 Nanoparticles and Nanoparticle Dimer Substrates. *Nano Letters* **2005**, *5*, (8), 1569-1574.
- 717 84. Huijbregts, M. A. J.; Hellweg, S.; Frischknecht, R.; Hendriks, H. W. M.; Hungerbühler,
718 K.; Hendriks, A. J., Cumulative Energy Demand As Predictor for the Environmental Burden of
719 Commodity Production. *Environmental Science & Technology* **2010**, *44*, (6), 2189-2196.
- 720 85. Huijbregts, M. A. J.; Rombouts, L. J. A.; Hellweg, S.; Frischknecht, R.; Hendriks, A. J.;
721 van de Meent, D.; Ragas, A. M. J.; Reijnders, L.; Struijs, J., Is Cumulative Fossil Energy
722 Demand a Useful Indicator for the Environmental Performance of Products? *Environmental*
723 *Science & Technology* **2006**, *40*, (3), 641-648.
- 724 86. Shibasaki, M.; Fischer, M.; Barthel, L., Effects on Life Cycle Assessment — Scale Up of
725 Processes. In *Advances in Life Cycle Engineering for Sustainable Manufacturing Businesses*,
726 Takata, S.; Umeda, Y., Eds. Springer London: 2007; pp 377-381.
- 727 87. Shibasaki, M.; Warburg, N.; Eyerer, P. In *Upscaling effect and Life Cycle Assessment*,
728 2006, 2006; 2006.

- 729 88. Caduff, M.; Huijbregts, M. A. J.; Althaus, H.-J.; Hendriks, A. J., Power-Law
730 Relationships for Estimating Mass, Fuel Consumption and Costs of Energy Conversion
731 Equipments. *Environmental Science & Technology* **2011**, *45*, (2), 751-754.
- 732 89. Caduff, M.; Huijbregts, M. A. J.; Koehler, A.; Althaus, H.-J.; Hellweg, S., Scaling
733 Relationships in Life Cycle Assessment. *Journal of Industrial Ecology* **2014**, *18*, (3), 393-406.
- 734
735
736

737

Table of Contents Figure (For TOC only)

738

739